

PERFORMANCE INVESTIGATION OF THREE-PHASE AND SINGLE-PHASE
E-CORE HYBRID EXCITATION FLUX SWITCHING MOTOR
FOR HYBRID ELECTRIC VEHICLE APPLICATIONS

SITI NUR UMIRA BINTI ZAKARIA

A project report submitted in partial
fulfillment of the requirement for the award of the
Degree in Master of Electrical Engineering with Honours

Faculty of Electrical and Electronics Engineering
University of Tun Hussein Onn Malaysia

JULY 2015

ABSTRACT

Research and development of hybrid electric vehicles (HEVs) which integrate battery-based electric motor with conventional internal combustion engine (ICE) has flourished since the last decade given their commitment in reducing green house effect and global warming. Although IPMSM is deemed as an effective electric motor used in HEVs, it's have some limitations such as distributed armature windings, uncontrollable permanent magnet (PM) flux, and higher rotor mechanical stress remain to be resolved. A new candidate of hybrid excitation flux switching motor (HE-FSM) at various rotor pole number such as 6S-4P, 6S-5P, 6S-7P, 6S-8P, 6S-14P, 4S-4P, 4S-6P 4S-8P and 4S-10P E-Core HE-FSMs, built on concentrated armature and DC field excitation (DC-FE) coil windings, variable flux capability with robust rotor structure which is suitable for high-speed operation is proposed and examined in this thesis. In this research, a commercial FEA solver, JMAG-Studio 13.0 released by JSOL Corporation, is used for 2D-FEA. JMAG was released as a tool to support design for devices such as motors, actuators, circuit components, and antennas. Design feasibility studies of E-Core HE-FSMs and deterministic optimization method have been applied to improve the proposed machine. The goal of this design is to achieve torque and power higher than 303Nm, 123kW and 101Nm, 41kW for three-phase and single-phase, respectively, so as to compete with the IPMSM commonly used in HEV. As a result, the maximum torque and power of the final design three phase and single-phase E-Core HE-FSMs are 313.29Nm, 260kW, 233Nm and 43.42kW respectively. Positively, the proposed HE-FSM has proved to be a good candidate for efficient and safe HEV drive.

ABSTRAK

Penyelidikan dan pembangunan kenderaan elektrik hibrid (HEVs) yang menggabungkan bateri-motor elektrik asas dengan enjin pembakaran dalaman konvensional (ICE) telah berkembang sejak sedekad yang lalu dan memberi komitmen dalam mengurangkan kesan rumah hijau serta pemanasan bumi. Walaupun IPMSM dianggap sebagai motor elektrik yang telah berjaya digunakan dalam HEVs, terdapat beberapa kekurangan seperti pertindihan penggulangan angker, fluks magnet (PM) yang tidak terkawal, dan tekanan mekanikal tinggi pada pemutar. Struktur baru pengujian fluks hibrid beralih motor (HE-FSM) pada pelbagai jumlah kutub pemutar seperti 6S-4P, 6S-5P, 6S-7P, 6S-8P, 6S-14P, 4S-4P, 4S-6P 4S-8P dan 4S-10P E-Core HE-FSMS, dibina dengan penggulangan angker dan pengujian medan (FE) bersebelahan dan struktur pemutar yang lasak sesuai untuk operasi kelajuan tinggi dicadangkan dan dibincangkan di dalam kajian ini. Dalam kajian ini, JMAG-Studio 13.0 dikeluarkan oleh JSOL Corporation, digunakan untuk 2D-FEA. JMAG merupakan alat untuk menyokong reka bentuk untuk peranti seperti motor, penggerak, komponen litar, dan antena. Kajian reka bentuk E-Core HE-FSMS dan kaedah pengoptimuman telah digunakan untuk meningkatkan prestasi mesin yang telah dicadangkan. Matlamat rekabentuk ini adalah mencapai daya tujah dan kuasa yang lebih tinggi daripada 303Nm, 123kW untuk tiga-fasa dan 101Nm, 41kW untuk fasa tunggal, bagi bersaing dengan IPMSM. Hasil daya tujah maksimum dan kuasa bagi struktur reka bentuk akhir masing-masing adalah 313.29Nm, 260kW bagi tiga fasa, dan 233Nm 43.42kW bagi fasa tunggal. Cadangan HE-FSM telah terbukti menjadi calon yang baik untuk memandu HEV cekap dan selamat.

CONTENTS

TITLE	i
DECLARATION	ii
DEDICATION	iii
ACKNOWLEDGEMENT	iv
ABSTRACT	v
ABSTRAK	vi
CONTENTS	vii
LIST OF TABLES	xi
LIST OF FIGURES	xii
LIST OF ABBREVIATIONS	xvi
CHAPTER 1 INTRODUCTION	1
1.1 Research background	1
1.2 Problem statement	2
1.3 Research objectives	3
1.4 Scope of project	3
1.5 Thesis outlines	4
CHAPTER 2 LITERATURE REVIEW	6
2.1 Introduction	6
2.2 Review on electric motor used in HEV	6

2.3	IPMSM used in HEV application	9
2.4	Classification of flux switching machine (FSM)	9
2.4.1	Permanent magnet flux switching machine (PM-FSM)	10
2.4.2	Field excitation flux switching machine (FE-FSM)	12
2.4.3	Hybrid Excitation flux switching machine (HE-FSM)	14
2.5	Topology of E-Core HE-FSM	16
2.6	Selected HE-FSM topology for HEV applications	19
2.6.1	Magnetic equivalent circuit	20
2.7	JMAG Designer	22
2.8	Summary	23
CHAPTER 3 METHODOLOGY		24
3.1	Introduction	24
3.2	Phase 1: Initial design method	24
3.3	Phase 2: Performance investigation method	27
3.3.1	Open circuit analysis	27
3.3.2	Short circuit analysis	29
3.4	Phase 3: Design improvement and optimization	29
3.5	Summary	30
CHAPTER 4 DESIGN OF THREE-PHASE E-CORE HE-FSM		31
4.1	Introduction	31
4.2	Three-phase E-core HEFSM at various rotor poles configuration	31
4.3	No load analysis	34
4.3.1	Armature coil arrangement test	34
4.3.2	Flux path of PM and DC-FE coil at open circuit condition, back-emf and cogging torque	35
4.3.3	DC-FE coil and PM with DC-FE coil flux linkages at varying J_e	38

4.4	Load analysis of the original E-core HE-FSM	39
4.4.1	Torque and power vs. speed characteristics	39
4.5	Design improvements of 6S-14P E-Core HE-FSM	41
4.5.1	Design parameter and procedures	42
4.6	Results and performance of the final Design of 6S-14P E-Core HE-FSM	49
4.6.1	Distribution of field flux by PM and DC-FE coil excitation, induced voltage waveforms and cogging torque	49
4.6.2	Torque and power factor vs. J_a and J_e Curves	50
4.6.3	Torque and Power vs. speed curves	53
4.6.4	Rotor Mechanical Stress	56
4.6.5	PM demagnetization	57
4.6.6	Loss prediction and motor efficiencies	58
4.7	Summary	61
 CHAPTER 5 DESIGN OF SINGLE-PHASE E-CORE HE-FSM		62
5.1	Introduction	62
5.2	Single-phase E-core HEFSM at various rotor poles configuration	62
5.3	No load analysis	65
5.4	Load analysis of single-phase E-Core HEFSM	68
5.5	Design optimization of 4S-10P E-Core HEFSM	69
5.5.1	Evolution of 4S-10P single-phase E-Core HE-FSM	73
5.6	Result and performance of final design 4S-10P single-phase 4S-10P E-Core HEFSM	74
5.6.1	Flux line of PM and DC-FE coil at open circuit condition	74
5.6.2	Torque versus DC-FE coil current density curve	76
5.6.3	Rotor mechanical stress	79
5.6.4	Torque and power versus speed curve	80
5.6.5	PM demagnetization	81

5.6.6	Motor losses and efficiencies	82
5.7	Summary	84
CHAPTER 6 CONCLUSION		85
6.1	Introduction	85
6.2	Conclusion	85
6.2	Recommendation and future work	86
REFERENCES		87

LIST OF TABLES

3.1	The details of combination between number of stator slots, N_s and number of rotor poles, N_r	27
4.1	Parameters of Initial and Improved Design 6S-14P E-Core HE-FSM	48
4.2	PM demagnetization at various temperatures	58
4.3	Motor efficiency of the final design 6S-14P E-Core HE-FSM	60
4.4	Overall performances of 6S-14P three phase E Core HE-FSM	61
5.1	Design restrictions and target performances of single-phase E-Core HE-FSM	64
5.2	Initial design parameters of 1- \emptyset E-Core HE-FSM	65
5.3	Parameter of initial and final of 4S-10P single-phase E-Core HE-FSM	72
5.4	Motor efficiency of the final design 4S-10P E-Core HE-FSM	83
5.5	Overall performances of the final design 4S-10P E Core HE-FSM	84

LIST OF FIGURES

2.1	IPMSM used in HEV	9
2.2	Classification of Flux Switching Machine (FSMs)	10
2.3	Examples of PM-FSMs	11
2.4	Principle operation of PM-FSM	11
2.5	Example of FE-FSMs	13
2.6	Principle operation of FE-FSM	13
2.7	Example of HE-FSMs	15
2.8	E-Core topologies	17
2.9	Operation of E-Core HE-FSM	19
2.10	Original design of 6S-14P and 4S-10P E-Core HE-FSM	20
2.11	Magnetic equivalent circuit	22
3.1	Work flow of electrical motor design	25
3.2	Initial Design parameter for E-Core HE-FSM	30
3.3	Optimization Process	30
4.1	Main machine dimension of the proposed E-Core HE-FS	33
4.2	Three-phase flux linkage of E-core HE-FSMs	34
4.3	Flux lines of dissimilar slot-pole combination	35
4.4	Flux path of PM with maximum DC-FE coil of $30\text{A}/\text{mm}^2$	36
4.5	Back-emf in various rotor pole configurations	37
4.6	Cogging torque of initial design E-core HE-FSMs	37
4.7	DC-FE coil flux linkage at various J_e	38
4.8	PM and DC-FE coil flux linkages at various J_e	38

4.9	Torque versus J_e at maximum J_a	40
4.10	Flux distribution of different slot-pole combinations	40
4.11	Torque versus speed E-core HE-FSM	41
4.12	Power versus speed E-core HE-FSM	41
4.13	Torque versus rotor radius D_1 characteristic	42
4.14	Torque vs. rotor pole width D_3 for various rotor pole depths D_2	43
4.15	Torque vs. DC-FE coil width D_7 for different DC-FE coil depth D_6	43
4.16	Improvement on E1	44
4.17	Improvement of E2 with PM=1.3, armature and DC-FE coil slot in rectangular shape	44
4.18	Improvement on E3	45
4.19	Improvement on E4	45
4.20	Improvement on E5	46
4.21	Bridge topology	47
4.22	Evolution of initial to optimum E-Core HE-FSM	47
4.23	Comparison of flux vector diagram three-phase E-Core HE-FSM designs	48
4.24	Flux path of the improve design	49
4.25	Back-emf of the initial and final design 6S-14P E-Core HE-FSM	50
4.26	Cogging torque of the initial and final design E-Core HE-FSM	50
4.27	Torque versus J_e at various J_a of the final design	51
4.28	DC-FE coil density vs. power factor curves	51
4.29	Torque and power factor of initial and improved design at max. J_a and J_e	53
4.30	Instantaneous torque profile for initial and final design	53
4.31	Comparison of torque vs. speed characteristic between E-Core HEFSM and IPMSM	54

4.32	Comparison of power vs. speed characteristic between E-Core HEFSM and IPMSM	54
4.33	Estimated coil end volume of the final design 6S-14P E-Core HE-FSM	55
4.34	Comparison of principal stress distributions of rotor at 20,000r/min	56
4.35	Flux contour diagram of PM at 180°C	57
4.36	Flux distribution of PM at 180°C	57
4.37	Maximum torque at various PM temperatures	58
4.38	Efficiency and motor losses at operating points	60
4.39	Iron loss and copper loss at operating points	60
5.1	Topology of single-phase E-Core HE-FSM	63
5.2	Flux linkage of 1- \emptyset E-Core HE-FSMs	66
5.3	Flux linkage of PM for single-phase E-Core HE-FSM	66
5.4	Back-emf at various rotor pole configurations	67
5.5	Cogging torque of the initial design	67
5.6	Flux linkage at various J_e	68
5.7	Torque versus J_e at maximum J_a	68
5.8	Flux density distribution	69
5.9	Torque versus D_1 , D_2 , and D_3 characteristic	70
5.10	Torque versus D_6 , D_7 characteristic	71
5.11	Torque versus D_8 , D_9 characteristic	71
5.12	Parameters of 4S-10P E-Core HE-FSM design	72
5.13	Cycle optimization of 4S-10P E-Core HE-FSM	72
5.14	Design optimization of 4S-10P E-Core HE-FSM	73
5.15	Comparison of torque and power at various E-Core HE-FSM designs	74
5.16	Flux path of the final design	75
5.17	Back-emf of the original and final design 4S-10P E-Core HE-FSM	75
5.18	Cogging torque of 4S-10P E-Core HE-FSM	76
5.19	Distribution of field flux formed by FE coil excitation position	77

5.20	Torque versus J_e at various J_a of the final design	78
5.21	Comparison of flux distribution between initial and final designs improved design	78
5.22	Instantaneous torque of initial and final design at max. J_a and J_e	79
5.23	Principal stress distributions of rotor at 20,000r/min	80
5.24	Comparison of torque vs. speed characteristics between initial and final design 4S-10P E-Core HE-FSM	81
5.25	Comparison of power vs. speed characteristics	81
5.26	Flux density contour diagram of permanent magnet for initial and final design	82
5.27	Efficiency and motor losses at operating points	83
5.28	Iron loss and copper loss at operating points	83

LIST OF ABBREVIATIONS

6S-14P	6 Slot 14 Pole
A	Ampere
AC	Alternating Current
C	Celsius
Dy	Dysprosium
DC	Direct Current
EV	Electric Vehicle
FEA	Finite Element Analysis
FE	Field Excitation
f_e	Electrical frequency
FE-FSM	Field Excitation Flux Switching Motor
f_m	Mechanical rotation frequency
HE-FSM	Hybrid Excitation Flux Switching Motor
HEV	Hybrid Electric Vehicle
IMs	Induction Motors
IPMSMs	Interior Permanent Magnet Synchronous Motors
ICE	Internal Combustion Engine
J_E	FEC current density
J_A	Armature coil current density
kg	Kilogram
kW	Kilowatt
mm	Millimeter
N_a	Number of turns for armature
N_e	Number of turns for excitation
Nm	Newton meter

Nd	Neodymium
PM	Permanent Magnet
PMFSM	Permanent Magnet Flux Switching Motor
r/min	Revolution per minute
S _a	Slot area
SRM	Switched Reluctance Motor
T	Tesla
Wb	Weber

CHAPTER 1

INTRODUCTION

1.1 Research background

For more than 100 years, vehicles equipped with conventional internal combustion engine (ICE) have been used for personal transportation. In recent days, with rapid increasing rates of world population, demands for private vehicles are also increasing. One of the serious problems associated with rising use of personal vehicles is the emissions. The enhanced greenhouse effect, also known as global warming, is an acute issue that all people have to face. Government agencies and organizations have developed more stringent standards for the fuel efficiency and emissions. In order to obtain a wide-range full-performance high efficiency vehicle while eliminating pollutant emissions, the most feasible solution at present is hybrid electrical vehicle (HEV) which driven by battery-based electric motor [1-5].

Selection of electric motor for HEV propulsion systems is very important step and requires special attention. In fact, the automotive industry is still seeking for the most appropriate electric-propulsion system for HEVs. In this case, the key features are efficiency, reliability and cost. The process of selecting the appropriate electric-propulsion systems should be carried out at the system level. Mainly, the choice of electric-propulsion systems for HEV depends on three factors; driver's expectation, vehicle design constraints, and energy source. With these considerations, it is understood that the specific motor operating points are difficult to define [6]. Hence, selecting the most appropriate electric-propulsion system for the HEV is always a challenging task. To date, several electric motors for HEV propulsion system under

great consideration are DC motor, induction motor (IM), switched reluctance motor (SRM), and permanent magnet synchronous motor (PMSM) [7]. Based on the exhaustive review on state of the art of electric-propulsion systems, it is observed that investigations on the cage IMs and the PMSMs are highly dominant, whereas those on dc motors are decreasing but SRMs are gaining much interest [8].

The major requirements of HEVs electric propulsion on electric motor drive are summarized as follows:

- (i) High instant power, high power density, high power at high speed for cruising.
- (ii) Fast torque response and high torque at low speed for starting and climbing.
- (iii) Very wide speed range, including constant-torque and constant-power regions
- (iv) High efficiency over the wide speed and torque ranges
- (v) High efficiency for regenerative braking
- (vi) High reliability, fault tolerant and robustness for various vehicle operating conditions.
- (vii) Downsizing, weight reduction, and lower moment of inertia
- (viii) Suppression of electromagnetic interference (EMI) of motor controller
- (ix) Market acceptance degree of each motor type, which is closely associated with the comparative availability of materials and cost of its associated power converter technology [9].

1.2 Problem statement

One example of successfully developed PMSM for HEV drives system is Interior PMSM (IPMSM) that has been installed in Toyota Prius, Estima Hybrid, Lexus RX400h and GS450h. In spite of their good performances and well operated in HEV systems, there are some disadvantages of IPMSM such as: [10]

- (i) The three-phase armature windings used in IPMSM are wound in the form of distributed windings which results high coil end length and increase in copper loss.
- (ii) The constant flux from PM is difficult to control especially at light load high speed operating points.
- (iii) The volume of rare-earth PM materials used in IPMSM is high,

approximately 1.3kg.

- (iv) The present IPMSM has a complex structure of PM and armature coil slots, thus difficult to manufacture and to optimize.
- (v) The mechanical stress of the rotor depends on the number of PM bridges. High number of bridges not only increases the mechanically weak points but also causes much flux leakage between the PMs that will degrade the performance of the machine.

1.3 Research objectives

In order to overcome the problems in 1.2, a new machine is identified and selected as the alternative candidate for HEV applications. Thus, the objectives of this research are listed as follow:

- (i) To propose and design a new structure of three-phase (3 \emptyset) and single-phase (1 \emptyset) E-Core HE-FSM.
- (ii) To investigate performances of E-Core HE-FSM at various rotor pole configurations under open and short circuit characteristics.
- (iii) To improve and optimize the three-phase (3 \emptyset) and single-phase (1 \emptyset) E-Core HE-FSM for HEV applications.

1.4 Scope of Project

The proposed 3-phase and 1-phase E-Core HE-FSMs are designed with similar geometrical dimensions and parameter specifications of IPMSM used in Toyota Prius [10] as reference using JMAG-Designer Ver.13.0. The outer diameter, the motor stack length, the shaft radius and the air gap of the main part of the machine design being 264mm, 70mm, 30mm and 0.8mm respectively. The electrical restrictions related with the inverter such as maximum 650V DC bus voltage and maximum 360V inverter current are set. Assuming water jacket system is employed as the cooling system for the machine, the limit of the current density is set to the maximum 30A_{rms}/mm² for armature winding and 30A/mm² for DC-FEC, respectively.

Initially, the operating principle of the proposed motor is investigated using coil arrangement test to ensure the three-phase and single-phase flux linkage generation, correspondingly. Then, performances of the proposed HE-FSMs for various rotor poles structures are analyzed at open circuit condition and short circuit condition such as coil test, flux linkage, induced voltage, cogging torque, power characteristics and torque versus speed profiles.

The three-phase 6S-14P and single-phase 4S-10P HE-FSMs are improved and optimized using deterministic optimization method until the target torque and power of more than 303Nm and 123kW, and 101Nm and 41kW for three-phase, single phase, respectively are achieved.

1.5 Thesis outlines

This thesis deals with the design studies on high power density hybrid excitation flux switching machine (HE-FSM) for HEV applications. The thesis is divided into 6 chapters and the summary of each chapter are listed as follows:

(i) Chapter 1: Introduction

The first chapter gives some introduction about the research including research background, related works on HEV and some explanation regarding IPMSM used in HEV. Then problems of current IPMSM used in HEV are highlighted and the research objectives and scope of the research are set to solve the problems. Besides, the design requirements, restrictions and specifications of the proposed E-Core HE-FSM with similar restriction and specifications of IPMSM used in HEV are also discussed.

(ii) Chapter 2: Overview of Flux Switching Machines (FSMs)

The second chapter explained some introduction and classifications of FSM including the example of PM-FSM, FE-FSM and HE-FSM, the operating principle and the proposed HE-FSM for HEV applications.

(iii) Chapter 3: Research methodology

The third chapter describes the process that involve to completing this research. The processes during this research are divided into several phases

including design process, optimization and analysis of the proposed E-Core HE-FSM.

(iv) Chapter 4: Design of three-phase E-Core HE-FSM

This chapter explains the performances of various combinations of slot-pole three-phase E-Core HE-FSMs such as 6S-4P, 6S-5P, 6S-7P, 6S-8P and 6S-14P using commercial 2D-FEA, JMAG-Studio ver. 13.0, released by JSOL Corporation. Since the initial performances are far from the target requirements of 303Nm and 123kW due to flux saturation between armature coil and DC-FE coil at high current density condition, design improvements using “deterministic optimization method” to treat several design parameters are conducted until the target performances are achieved. The comparison between the initial and final design 6S-14P three-phase E-Core HE-FSM is discussed.

(v) Chapter 5: Design of single-phase E-Core HE-FSM

This chapter, a single-phase E-Core HE-FSM is proposed as one of suitable candidate to be applied for small EV/HEV applications such as Honda Jazz, Nissan Leaf and Toyota Prius. Single-phase motor in real EV/HEV drive system are much smaller converter size, smaller battery package due to small voltage capacity when compared with the three-phase system. The design specifications, restrictions and target performances are similar with 6S-14P HE-FSM as discussed in Chapter 1. The similar “deterministic optimization method” is used to treat several parameters in effort to achieve the target performances. All final designs with optimum performances are compared and summarized.

(vi) Chapter 6: Conclusion and future work

The final chapter presents the summary and conclusion of the research and pointed out some future works for design improvements.

CHAPTER 2

LITERATURE REVIEW

2.1 Introduction

The emphasis on green technology is highly demanded in modern cities. The significant growth of today's cities has led to increase use of transportation, which brings about aggravated urban pollution and other serious environmental issues such as the greenhouse effect that culminates in global warming. Gases produced by vehicles should be strictly controlled and proactive measures must be taken to minimize these deleterious emissions [11]. Japan was the first country to commercialize HEV since the interest of tackling environmental problems [12]. IPMSM is an example of successfully developed electric motor for HEVs which utilizes rare-earth PM commonly employed to increase power density of the machine [13-14]. However, to address the weaknesses of IPMSM, a new HE-FSM is built. The first concept of flux switching machine (FSM) was founded and published in the mid-1950s [15]. Over the last ten years, many novel and new FSMs topologies have been proposed for various applications, ranging from low cost domestic appliances, automotive, wind power, aerospace, and traction drive applications, etc.

2.2 Review on electric motor used in HEV

Driven by concern about the environment, automakers, government, and automobile users retain a keen interest in HEV, which makes the research in this area intriguing. As electric motors are the core of HEV, there is a pressing need for researchers to develop advanced, state-of-the-art electric motors [16, 17]. To date, HEV is known to be the most promising green vehicle built with a combination of electric traction motors and internal combustion engine (ICE). The four candidates of electric motors

for HEV that has been mentioned previously are DC motor, induction motor (IM), switch reluctance motor (SRM), and permanent magnet synchronous motor (PMSM).

DC motor is most widely applied in as much as it requires only the DC supply. Besides, it abides by the principle of simple control based on the orthogonal disposition of field and armature mmf. DC motors have been prominent in electric propulsion system due to their torque-speed characteristics that suit the traction requirements and their control of the orthogonal disposition of field and armature mmf is simple. However, due to the use of commutator and brush, DC drive encounters a vital problem which renders it unsuitable and less reliable for maintenance-free drive [18-20]. To that end, researchers have explored the possibility of applying IM which is a non-PM motor for electric propulsion of HEV. In general, IM is reliable, cost-effective, rugged, and capable of operating in harsh surroundings. Overall, it requires low maintenance. Nonetheless, its relatively low efficiency in the low speed, light load region of HEV thus a result of secondary loss may affect fuel consumption and degrade system efficiency. Furthermore, IM drive has such drawback as necessity for high electric loading to achieve high torque density and low power factor. This stringent requirement poses a difficult challenge for large motor, thus eliminating IM from being a candidate for HEV's electric propulsion system [21].

As for SRM, it is a non-PM motor recognized to have great potential for HEV drive applications. Its advantages include simple and rugged construction, low manufacturing cost, fault tolerance, easy control, and excellent torque-speed characteristics. On the whole, SRM can operate at extremely broad constant power range. Yet, it is at a disadvantage and drops out of the race owing to vibration issue, large torque pulsation, acoustic noise which necessitates special converter topology, excessive bus current ripple, and electromagnetic interference that generates unwanted noise [22-25]. Acceptable solutions to the above disadvantages are needed to get a viable SRM-based EV [26]. On the other hand, PMSMs where the main flux is supplied by permanent magnet (PM) only are becoming more attractive and most capable of competing with other motors for the electric propulsion of HEVs. In fact, they are adopted by well-known automakers such as Toyota, Honda, etc., for their HEVs. These motors have many advantages. The overall weight and volume are significantly reduced for a given output power, and it has high power density, high

efficiency and high reliability. In addition, the heat generated can be efficiently dissipated to the surroundings. However, due to their limited field weakening capability, these motors are difficult to extend constant power speed region, as the presence of the fixed PM magnetic field. In order to extend the constant power speed range and improve the efficiency of PMSMs, the power converter can be controlled by six-pulse operation at above the base speed. The speed range may be extended three to four times over the base speed. To realize the wide speed ranges in these motors, an additional dc field excitation (DC-FE) coil winding is introduced, in such a way that the air-gap field provided by PMs can be weakened during a high-speed constant-power operation by controlling the direction and magnitude of the dc field current which are also called PM hybrid motors.

However, at a very high-speed range, the efficiency may drop because of increase in iron loss and also there is a risk of PM demagnetization [7-9]. There are various configurations of the PMSMs which can be classified as surface PMSM (SPMSM) and interior PMSM (IPMSM). The latter is more mechanically rugged due to the embedded PM in the rotor. Although, the SPMSM design uses fewer magnets than the IPMSM, both the motors may achieve a higher air-gap flux density. Another configuration of PMSM is the PM hybrid motor, where the air-gap magnetic field is obtained from the combination of PM and DC-FE coil as mentioned previously. In the broader term, PM hybrid motor may also include the motor whose configuration utilize the combination of PMSM and SRM. Although the PM hybrid motor offers a wide speed range and a high overall efficiency, the construction of the motor is more complex than PMSM. In other literatures, the PMSM is also particularly suited for the wheel direct-drive motor applications as in [27]. In addition, a PMSM drives for HEV applications is explained in [28], while the electric motor drive selection issues for HEV applications is also discussed in [29-30]. In contrast, PMSM is brushless and has numerous attractive features compared with IPMSM employed conventionally in HEV. For PMSM, the volume of permanent magnet is reduced by approximately 50% of that in IPMSM, yet keeping the power density intact [31]. Hitherto, IPMSM maintains its competitive advantage over other motors with regard to electric propulsion of HEV.

2.3 IPMSM used in HEV application

The well-known automakers such as GM, BMW, Renault-Nissan, Toyota, Honda and so forth have long adopted IPMSM in view of its merits of lighter weight, lesser size, high power density, high torque, high reliability, and high efficiency. One example of successfully developed IPMSM as shown in Figure 2.1 was installed on Lexus RX400h in 2005 [32]. The historical progress in the power density of main traction motor installed on Toyota EVs show that the power density of each motor employed in Lexus RX400h'05 and GS450h'06 has been improved approximately five times and more, respectively, when compared with Prius'97 [33]. Although the torque density of each motor has been hardly changed, a reduction gear has enabled to elevate the axle torque necessary for propelling the large vehicles such as RX400h and GS450h. As one of effective strategies for increasing the motor power density, the technological tendency to employ the combination of a high-speed machine and a reduction gear would be accelerated.

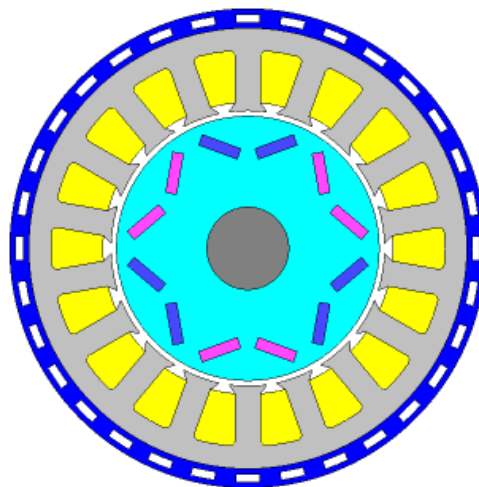


Figure 2.1: IPMSM used in HEV

2.4 Classification of Flux Switching Machine (FSM)

FSM can be categorized into three groups that are permanent magnet flux switching motor (PM-FSM), field excitation flux switching motor (FE-FSM), and hybrid excitation flux switching motor (HE-FSM).

Both PM-FSM and FE-FSM has only PM and DC field excitation (DC-FE) coil, respectively as their main flux sources, while HE-FSM combines both PM and FE coil as their main flux sources. Figure 2.2 illustrates general classification of FSM.

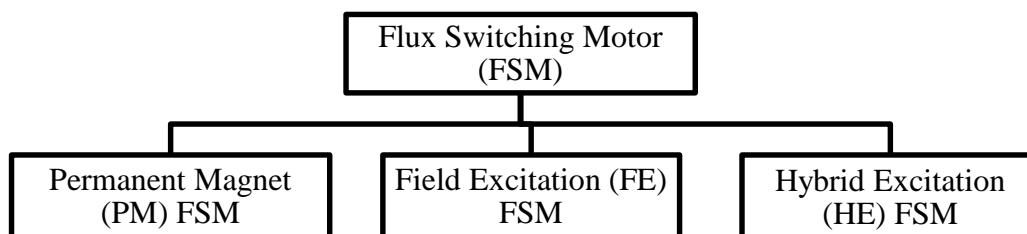


Figure 2.2: Classification of Flux Switching Machine (FSMs)

2.4.1 Permanent Magnet Flux Switching Machine (PM-FSM)

PM machine based on the principle of flux switching have been studied for several decades. Generally, such machines have a salient pole rotor and the PMs which are housed in the stator. A three-phase FSM based on the homo-polar flux principle and the bipolar flux principle have been described in [34] and [35], respectively, while a new type of single phase and three-phase PM-FSM in which a pair of PMs is embedded on the stator were reported in [36] and [37], respectively. In addition, the performance of Law's relay, a flux-switching type of limited angle actuator was proposed in [38].

Various examples of three-phase PM-FSM are illustrated in Figure 2.3. The multi-tooth structure is evolved from the C-core 6S-10P PM-FSM to improve the torque density and the PM usage as shown in Figure 2.3(a). In the figure, the number of rotor teeth is exactly double when compared with the previous PM-FSMs. The end of stator tooth is divided into two parts so that the flux can easily flow to all rotor teeth. However, as the demerits of this multi-tooth PM-FSM is high rotor pole numbers, the supply frequency of inverter will also be doubled when compared with the original design. Finally, a three-phase 12S-10P PM-FSM with segmental rotor is also reported as shown in Figure 2.3(b) [39]. The stator part consists of armature coil and PM while the rotor is divided into six U shape segments embedded into the shaft steel. The

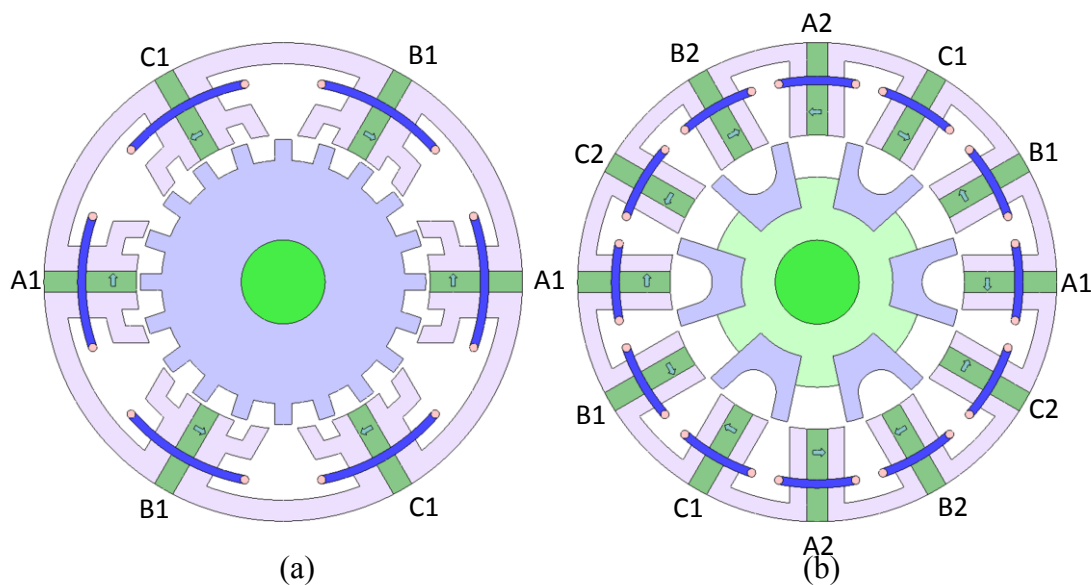


Figure 2.3: Examples of PM-FSMs (a) 6S-10P Multi-tooth PM-FSM (b) 12S-10P Segmental rotor PM-FSM

problem of such kind of machine is the rotor mechanical strength which needs to be considered.

The general operating principle of the PM-FSM is illustrated in Figure 2.4, where the red arrows show the flux line of PM as an example. From the figure, when the relative position of the rotor poles and a particular stator tooth are as in Figure 2.4(a), the flux-linkage corresponds to one polarity. However, the polarity of the flux-linkage reverses as the relative position of the rotor poles and the stator tooth changes as shown in Figure 2.4(b), i.e., the flux linkage switches polarity as the salient pole rotor rotates.

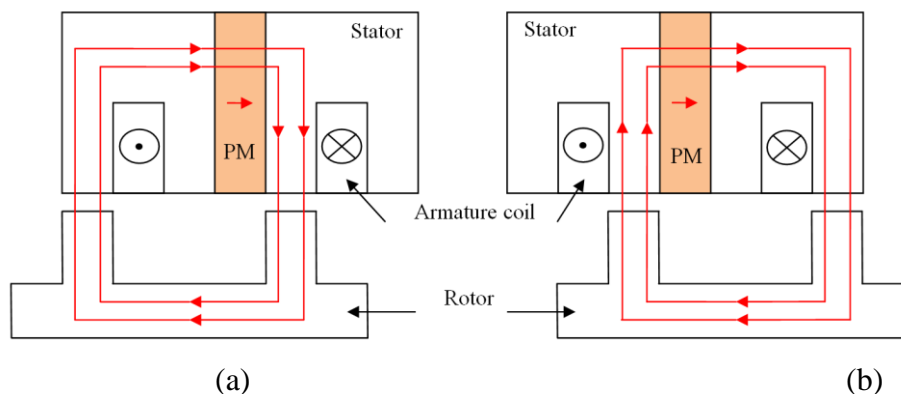


Figure 2.4: Principle operation of PM-FSM

2.4.2 Field Excitation Flux Switching Machine (FE-FSM)

The PM excitation on the stator of conventional PM-FSM can be easily replaced by DC-FE coil excitation on the stator, thereby bringing forth FE-FSM as depicted in Figure 2.5. Briefly, FE-FSM principle is based on switching the flux polarity linking with the armature coil windings by changing the rotor position. Figure 2.5(a) is an example of single-phase four-stator-slot and two-rotor-pole (4S-2P) FE-SFM composed of a DC-FE coil, a toothed rotor structure, and fully-pitched windings on the stator [40]. As clearly shown, the stator contains two armature coils and a DC-FE coil that overlap. The feasibility of this design has been verified in different applications requiring high power density with a good level of durability [41] and [42].

The novelty of this design is that the single-phase AC arrangement can be realized by application of DC-FE coil and armature windings to provide the desired flux orientation for rotation. The required torque is generated by variable mutual inductance of windings. Indeed, the single-phase FE-FSM coupled with a power electronic controller is easy to manufacture and has the virtue of very low cost yet impressively high throughput. Moreover, being an electronically commutated brushless machine, it has longer lifespan, is flexible, and allows accurate control of torque, speed, and position at no extra cost as compared with other machines. Even so, the single-phase FE-FSM has some deficiencies which is low starting torque, fixed direction of rotation, large torque ripple, and overlapping windings between armature coil and DC-FE coil.

To meet the rigid performance requirements of FE-FSM, the three-phase 12S-8P FE-FSMs with segmental rotor are developed as shown in Figure 2.5(b). Whereas segmental rotors are used traditionally to control the saliency ratio in synchronous reluctance machines (SynRM), the primary function of the segments in this design is to provide a defined magnetic path for conveying the field flux to adjacent stator armature coils as the rotor rotates. This design gives shorter end windings than the toothed rotor structure which is associated with overlapping coils. There are significant gains with this arrangement as it uses less conductor materials and also can improve the overall motor efficiency.

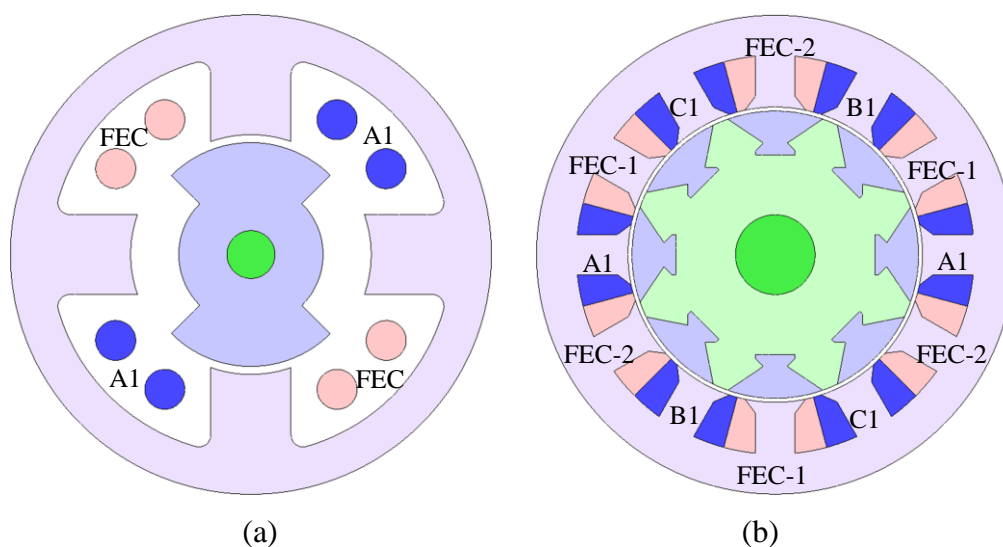


Figure 2.5: Example of FE-FSMs (a) 1-phase 4S-2P FE-FSM
(b) 3-phase 12S-8P segmental rotor FE-FSM

The working principle of FE-FSM is depicted in Figure 2.6. According to right-hand grip rule, Figures 2.6(a) and 2.6(b) indicate the flux direction of DC-FE coil into the rotor while Figures 2.6(c) and 2.6(d) illustrate the flux direction of DC-FE coil into

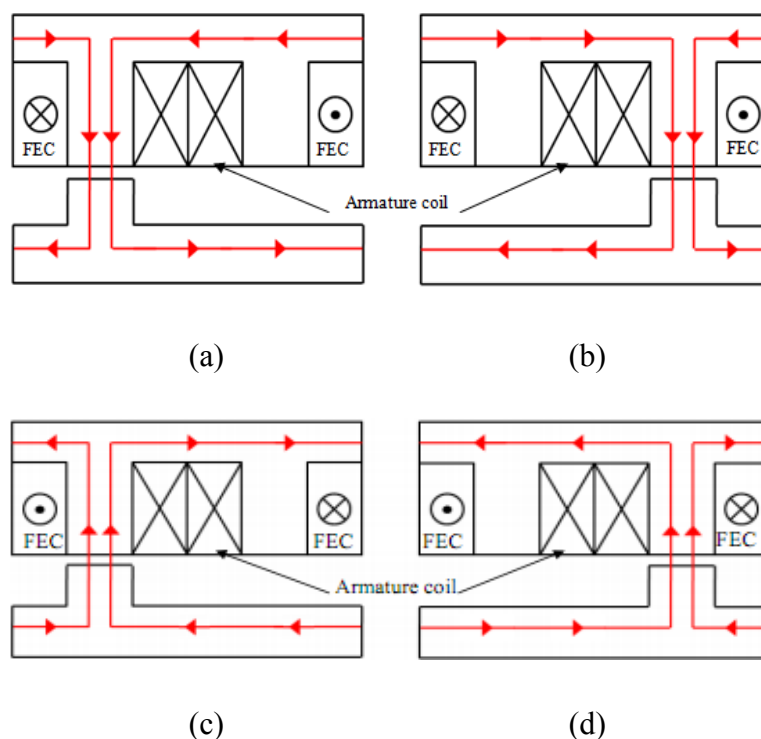


Figure 2.6: Principle operation of FE-FSM (a) $\theta_e=0^\circ$ and (b) $\theta_e=180^\circ$ flux moves from stator to rotor (c) $\theta_e=0^\circ$ and (d) $\theta_e=180^\circ$ flux moves from rotor to stator

the stator to produce a complete flux cycle. The combination of both fluxes forms the flux linkage at three-phase armature coil. With appropriate timing of armature current supply which is usually at zero rotor position of DC-FE coil flux for optimum performance the armature flux generated reacts with DC-FE coil flux to force the rotor to rotate continuously at a speed controlled by the armature current frequency. The DC-FE coil flux does not rotate but shifts clockwise or counter clockwise following the movement of salient pole rotor which coins the term “flux switching”.

2.4.3 Hybrid Excitation Flux Switching Machine (HE-FSM)

Hybrid excitation flux switching machines (HE-FSMs) exploits primary excitation by PM as well as DC-FE coil as secondary source. Conventionally, PM-FSMs can be operated beyond base speed in the flux weakening region by means of controlling the armature winding current. By applying negative d-axis current, the PM flux can be counteracted but with the disadvantage of increase in copper loss and thereby reducing the efficiency, reduced power capability, and also possible irreversible demagnetization of the PMs. Thus, HE-FSM is the underlying purpose of using two excitation field sources is to combine the advantages of PM-excited machine and DC-FE coil synchronous machine. Importantly, DC-FE coil controls excitation flux in the air gap, which strengthens flux weakening capability.

In effect, hybrid excitation by manipulating excitation flux enables designing a machine with relatively low armature magnetic reaction while extending the speed operation range. Furthermore, it improves efficiency in the most frequent operating zones of the traction motor. In general, machines with low armature magnetic reaction have better power factor, implying a lower power rating for the power converters connected to them. What is more, hybrid excitation allows additional degree of freedom and increases energy efficiency of the traction motor [43].

Various combinations of stator slots and rotor poles for HE-FSMs have been developed as illustrated in Figure 2.7. However, the machine has low torque density and long end winding for the DC-FE coils, which overlaps the armature windings, and increase copper loss. Moreover, based on the topology of a purely PM excited PM-FSM in Figure 2.3(a), a novel 12S-10P HE-FSM is developed [37], in which the PMs

dimensions are reduced to save space for the introduced DC-FE coil windings, whilst both the stator and rotor laminations are unchanged as depicted in Figure 2.7(b). It should be emphasized that the flux regulation capability of the machine can be simply controlled by adjusting the PM length in radial direction.

Meanwhile, the HE-FSM shown in Figure 2.7(b) is a 3-phase 12S-10P PM-FSM which incorporates the DC-FE coil at outer extremity of the stator [38]. However, the outer diameter of the machine is significantly enlarged for the DC-FE coil winding, which in turn reduces torque density. In addition, the PMs in the PM-FSM can be partially replaced by the DC-FE coil windings and consequently, several HE-FSM topologies were developed as in [38]. Although they have no overlapped between the armature coil and DC-FE coil, the torque capability is significantly reduced due to less PM volume. The foregoing HE-FSMs having magnets on the stator also suffers from one of three disadvantages.

- (i) The DC-FE coil is in series with the field excited by PMs, which limits the flux adjusting capability due to low permeability of the PM.
- (ii) The flux path of DC-FE coil significantly reduces the main flux excited by magnets and even short circuits the magnet flux.
- (iii) Torque density may be significantly reduced due to less PM volume.

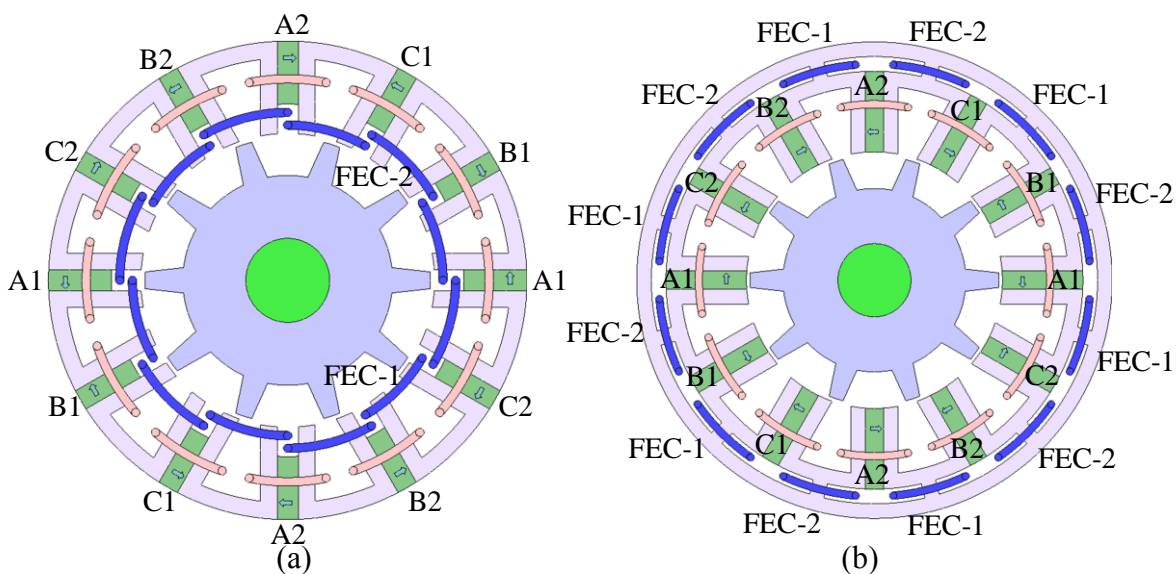


Figure 2.7: Example of HE-FSMs (a) 12S-10P Inner DC-FE coil HE-FSM
(b) 12S-10P Outer DC-FE coil HE-FSM

Furthermore, it is clear that to realize the hybrid topology of Figure 2.6(b), both PM and armature coil volume should be sacrificed while keeping the machine stator outer radius as constant. From the conventional PM-FSM topology, it is possible to replace some of the magnet material with DC-FE coils and therefore create several HE-FSM topologies without loss of armature coil. This represents the simplest method of hybridizing the conventional PM-FSM topology with DC-FE coil as it retains the existing stator and rotor dimensions and structure.

However, the HE-FSMs in Figure 2.7 (a) and (b) has a PM along the radial of the stator, thus the flux of PM in the outer stator acts as a leakage flux and has no contribution towards the torque production which reduces the machine performance. In addition, due to segmented stator core, the machine design is also difficult to manufacture. Furthermore the 12S-10P HE-FSM in Figure 2.6(b) has a complex structure, high volume of PM, consist of much armature coil and DC-FE coil that will degraded the efficiency at high current condition. Whereas, the new structure E-core HE-FSM with less PM volume, simple structure and also less volume of copper used in armature coil and DC-FE coil is proposed. Thus the machine efficiency is expected to be much higher when compared to other design. This machine is considered as the best candidate and is has been selected for further design improvement for HEV applications in this research.

2.5 Topology of E-Core HE-FSM

The development of E-Core HE-FSM started with evolution of the conventional 12S-10P permanent magnet flux switching machine (PM-FSM), as illustrated by Figure 2.8. In Figure 2.8(a), the salient pole stator core consists of modular ‘U-shaped’ laminated segments which are placed circumferentially between alternate polarities of magnetized PMs. The stator winding comprises concentrated armature coils wound around stator pole formed by two adjacent laminated segments and a magnet. Compared with conventional brushless PM machine [44], the slot area is reduced upon moving the magnet from rotor to stator. Moreover, the magnet-induced rise in temperature becomes easily manageable with a liquid cooling system, since heat can hardly be dissipated from rotor of a conventional machine.

As depicted in Figures 2.8(a) and 2.8(b), PM-FSM may have poles uninterruptedly or alternately wound. For the latter configuration, torque declines considerably when PM is eliminated from the stator poles without coils. In order to minimize the use of PM, and consequently the cost, the stator poles without coils are replaced by corresponding stator teeth. As PMs in the stator poles which carry coils are magnetized in the same direction, their magnetic fields are ‘short-circuited’ via stator back-yoke. For that reason, the circumferentially magnetized magnets of alternate polarities are employed instead, as shown in Figure 2.8(c). It is designated as E-Core PM-FSM due to its ‘E-shaped’ laminated segments in the stator. In contrast to

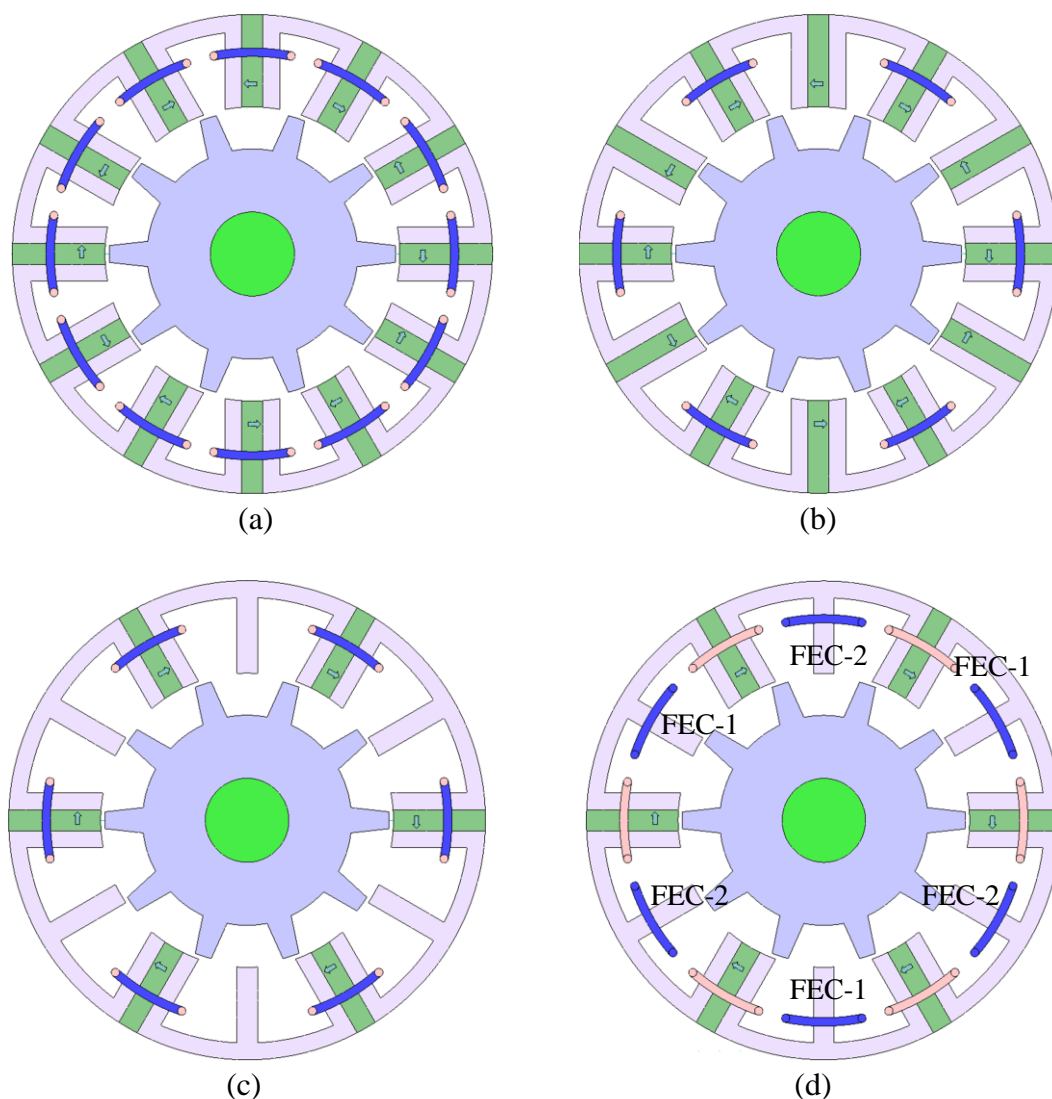


Figure 2.8: E-Core topologies: (a) Conventional PM-FSM with uninterruptedly wound poles (b) Conventional PM-FSM with alternately wound poles (c) E-Core PM-FSM with alternate PM directions (d) E-Core HE-FSM

conventional PM-FSM with uninterruptedly wound poles, E-Core PM-FSM which keeps the same rotor structure has less number of stator poles and half-sized PM. Together, the magnet and its two adjacent stator teeth define each stator pole [18] and [45].

Figure 2.8(d) introduces a new structure of 6S-10P E-Core HE-FSM specially designed with additional DC-FE coils on the in-between stator teeth of E-Core PM-FSM without magnet [46]. It retains the outer diameter of an analogous E-Core PM-FSM and exhibits simpler 2D structure as compared with a hybrid excitation PM machine developed from conventional PM-FSM. Since E-Core HE-FSM applies non-overlapping strategy between DC-FE coil and armature windings, its number of turns per phase is the same as that of E-Core PM-FSM. In addition, the slot area of this motor is partitioned into two parts—armature coil and DC-FE coil windings. Given their comparable slot areas, the total number of winding turns for armature is made equal to that of DC-FE coil to facilitate comparison of armature and field currents. Being distinct from HE-FSM built on conventional PM-FSM [47], the magnetic field excited in this carefully designed E-Core HE-FSM is similar to that in E-Core PM-FSM. With additional DC-FE coil, E-Core HE-FSM can conveniently incorporate the variable flux control capability, as opposed to constant flux of PM-FSM that limits its applications.

The operating principle of the proposed E-core HE-FSM is similar with conventional flux switching machine (FSM) in which the flux flows from the stator to the rotor switches its polarity following the rotation of rotor. At one instant, half of rotor poles receive the flux from the stator while another half of rotor poles bring the flux to the stator to make a complete flux cycle. The operating principle and definition of flux switching can be described either by changing flux in the stator or changing flux in the rotor. Figure 2.9 illustrates the operating principle of E-Core HE-FSM in three different conditions where the red and blue line indicate the flux from PM and FEC, respectively. In Figure 2.9(a), both fluxes of PM and DC-FE coil flow from stator to rotor pole P2 and return back to the stator by rotor pole P1. At this stage, it is obvious that rotor pole P2 received the flux from stator.

Meanwhile, as the rotor moves approximately half electric cycle to the left (see Figure 2.9(b)), both fluxes flow from stator to rotor pole P3 in between DC-FE coil winding on the right hand side. At this stage, stator flux switches its polarity through

rotor pole P3 as receiving flux while rotor pole P2 sends flux back to the stator to form a complete flux cycle. Subsequently, as portrayed in Figure 2.9(c), we observe a condition in which rotor pole P3 takes the role of rotor pole P2 as depicted in Figure 2.9(a) to form one electric cycle.

In other words, the flux flows from stator to rotor pole P3 through stator teeth between PM and armature coil, whereas rotor pole P2 simultaneously brings the flux back to the stator. Since PM and DC-FE coil fluxes are directed in the same polarity, they add up and travel together into the rotor, producing a collective flux dubbed the hybrid excitation flux [48].

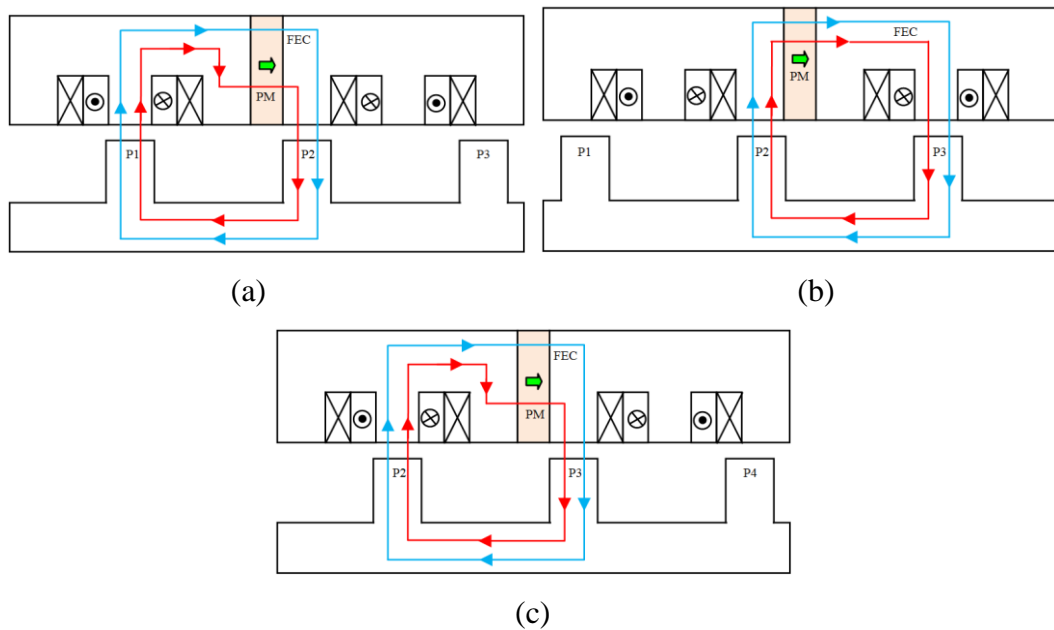


Figure 2.9: Operation of E-Core HE-FSM: (a) Flux flow via P2 and P1, (b) flux flow via P3 and P2, (c) flux flow via P3 and P2 to form one electric cycle.

2.6 Selected HE-FSM topology for HEV applications

In this thesis, based on the topology of HE-FSM discussed in Figure 2.8(d), a new design 6S-14P three-phase and 4S-10P single-phase E-Core HE-FSM as illustrated in Figure 2.10 is selected and proposed for HEV applications. Some design studies are conducted in the proposed design E-Core HE-FSM in effort to achieve the target performances of HEV considering design constraints and specifications of IPMSM used in Lexus RX400h [19]. From the figure, it is obvious that the proposed 6S-14P

E-Core HE-FSM is composed of 6 PMs and 6 pair of DC-FE coils slot, distributed uniformly in the midst of each armature coil. The term, “flux switching”, is coined to describe that the stator tooth flux switches its polarity by following the motion of a salient pole rotor. In this machine, the PMs and DC-FE coils produce six north poles interspersed between six south poles while the three-phase armature coils are accommodated in the 6 slots.

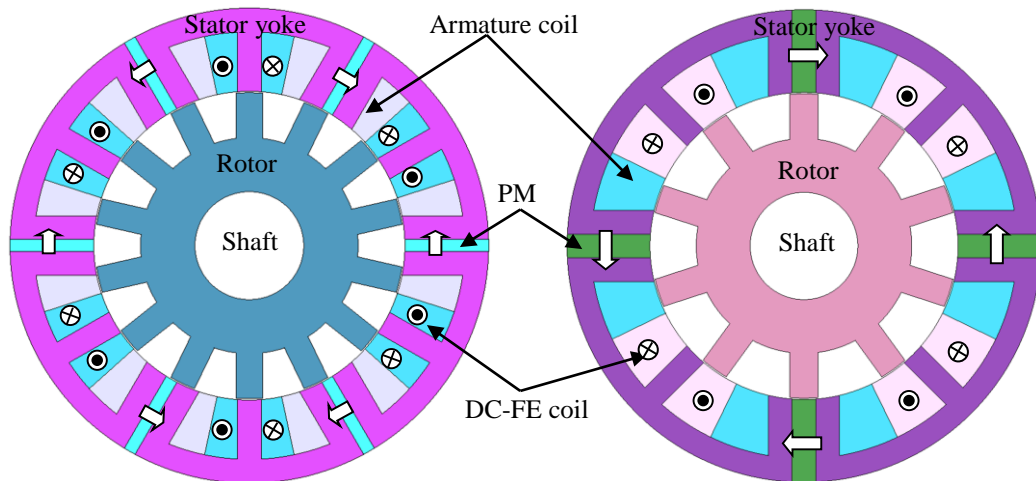


Figure 2.10: Original design of 6S-14P three-phase and 4S-10P single-phase E-Core HE-FSM

2.6.1 Magnetic equivalent circuit

The magnetic equivalent circuit (MEC) method is based on the analogies of the quantity relations in a magnetic field and in a resistive electric circuit [49], as shown in (2.1).

$$\phi \frac{F}{R} = F \cdot \mathcal{P} \quad (2.1)$$

In which Φ is the flux, F is the magnetomotive force (mmf), R is the reluctance and \mathcal{P} is the permeance.

Elements exist in a MEC can be categorized into two which are active elements as sources and passive elements as reluctances. Sources can be further classified into mmf and flux sources. Usually, the current-carrying coils are modeled as mmf sources in a MEC, since its mmf can be easily determined by Ampere's law. Permanent magnets are modeled as mmf sources with reluctance/permeance in series or flux sources with reluctance/permeance in parallel.

A stator MEC module is defined as the MEC model that represents the magnetic flux distribution in a unit section of stator, i.e. the section between central axes of each two neighbouring stator slots and the resulting MEC module is shown in Figure 2.11(a). In this module, the permanent magnet in the stator section is modeled as an mmf source F_{pm} with a permeance P_{pm} in parallel. The flux paths in the stator tooth and the stator back iron are modelled as different flux tubes with permeances P_{st} and P_{si} , respectively. The leakage flux outside the stator is also included and modelled as two parallel flux tubes with permeances P_{sl1} and P_{sl2} , respectively, as can be seen in Figure 2.11(a). Whereas the flux path for FE coil slot are modeled as P_{fe} as clearly represent in Figure 2.11(b)

Thus for general HEFSM, the reluctance network of stator consists of number of stator MEC modules that are similar to Figure 2.11(a). However, when connecting the circuits, the polarity of the mmf source should be reversed in each neighbouring module. Furthermore, it is worth noting that the actual magnetic flux paths in the stator vary with the rotor position. However, to simplify the modelling problem, this variation is neglected as the permeability of the ferromagnetic material is relatively large under non-saturated conditions.

A rotor MEC module is defined as the MEC model that represents the magnetic flux distribution in a unit section of rotor. This rotor section is obtained by dividing the rotor of the FSM into equal sections, each with a rotor tooth in the middle and the resulting MEC module is shown in Figure 2.11(c). In this module, the flux paths in the rotor tooth and the rotor back iron are modelled as different flux tubes with permeances P_{rt} and P_{ri} , respectively. For the general HEFSM, the reluctance network of rotor consists of number of rotor MEC modules. With the same simplifications as applied to the stator MEC modules, the rotor MEC modules are also assumed to be invariant to the rotor position.

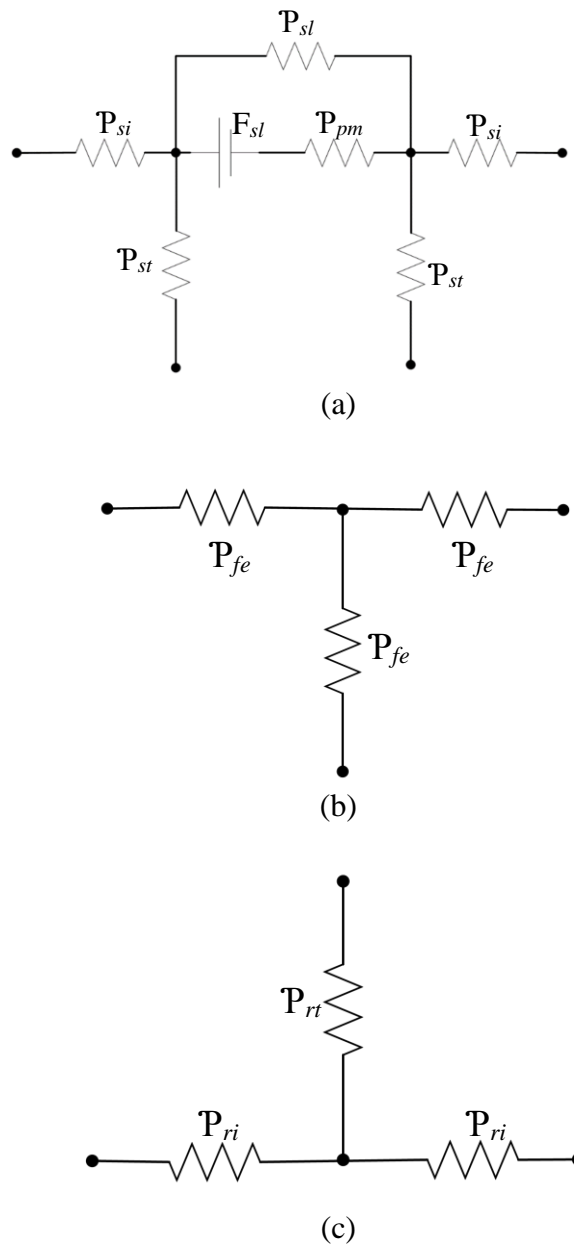


Figure 2.11: Magnetic equivalent circuit for (a) stator section (b) FE coil (c) rotor section

2.7 JMAG Designer

JMAG Designer is the high-speed, high-precision FEA software tool at the core of JMAG for electromechanical design. It is also an intuitive interface and precise modeling technology with a wide variety of results displays are built in. Since 1983, JMAG become a standard tool in EV/HV development. There are a lot of analysis modules in JMAG such as magnetic, electric, structural, thermal, multi-physics and

etc. besides, there are numerous analysis tools in JMAG designer software such as inductance calculation, parametric analysis, optimization, and scripting.

2.8 Summary

In this chapter, the overview and classifications of various FSMs are discussed. The PM-FSM, FE-FSM and HE-FSM have their own advantages and disadvantages which requires further investigations to extract higher performances for several applications. The best candidate of 6S-14P three-phase and 4S-10P single-phase E-Core HE-FSM is proposed for further design improvement in HEV applications as discussed in Chapter 4 and Chapter 5 respectively.

CHAPTER 3

METHODOLOGY

3.1 Introduction

This chapter discusses the methodology used in this research. This methodology plays an important role in implementing this research study accordingly. The project methodology is divided into several phases including design process, analysis and optimization of the proposed three-phase and single-phase E-Core HE-FSM as illustrated in Figure 3.1. It is obvious that the details of each design phase are described in this chapter, subsequently. Set design restrictions and specifications of the E-Core HE-FSM including main machine dimension, electrical restrictions and target performances as listed in Chapter 1. Commercial FEA package, JMAG-Designer ver.13.0, released by Japan Research Institute (JRI) is used as 2D-FEA solver for this design.

3.2 Phase 1: Initial design method

Geometry editor is used to design each part of motor separately such as rotor, stator, armature coil, and DC-FE coil. The main geometrical dimensions are based on IPMSM in which the stator outer diameter, stack length and shaft are set respectively to 132mm, 70mm and 30mm. To ensure flux flow from stator to rotor equally without any flux leakage, the rotor and stator tooth of the proposed machine is defined in Equation 3.1.

$$\sum \text{Stator Tooth Width} = \sum \text{Rotor Tooth Width} \quad (3.1)$$

REFERENCES

- [1] C. C. Chan, "The state of the art of electric, hybrid, and fuel cell vehicles", Proc. IEEE, vol. 95, no. 4, pp.704–718, Apr. 2007.
- [2] M. Ehsani, Y. Gao, and J. M. Miller: "Hybrid electric vehicles: architecture and motor drives", Proc. IEEE, Vol. 95, No. 4, pp.719–728, Apr 2011.
- [3] D. W. Gao, C. Mi, and A. Emadi: "Modeling and simulation of electric and hybrid vehicles", Proc. IEEE, Vol. 95, No. 4, pp.729–745, Apr 2009.
- [4] G. Rizzoni, L. Guzzella, and B. M. Baumann: "Unified modeling of hybrid electric vehicle drive trains", IEEE Trans. on Mechatronics, Vol. 4, No.3 pp.246–257, Sept. 1999
- [5] E. Sulaiman, T. Kosaka, and N. Matsui: "Design optimization and performance of a novel 6-Slot 5-Pole PMFSM with hybrid excitation for hybrid electric vehicle" IEEJ Transaction on Industry Application, Vol. 132 / No. 2 / Sec. D pp. 211-218, Jan 2012.
- [6] Z. Rahman, M. Ehsani, and K. Butler: "An Investigation of Electric Motor Drive Characteristics for EV and HEV Propulsion Systems," SAE Technical Paper, 2000.
- [7] L. Eudy, and J. Zuboy: "Overview of advanced technology transportation", National Renewable Energy Lab., U.S, Aug. 2004.
- [8] C. C. Chan: "The state of the art of electric and hybrid vehicles," Proc. IEEE, vol. 90, no. 2, pp.247–275, Feb. 2012.
- [9] T. M. Jahns, and V. Blasko: "Recent advances in power electronics technology for industrial and traction machine drives," Proc. IEEE, vol. 89, no. 6, pp.963–975, June 2011
- [10] M. Kamiya: "Development of traction drive motors for the Toyota hybrid systems", IEEJ Transaction on Industry Applications, vol.126, no.4, pp.473-479, April 2010

- [11] A. K. Yadav, P. Gaur, S. K. J ha, J.R.P. Gupta and A. P. Mittal, “Optimal Speed Control of Hybrid Electric Vehicles”, *Journal of Power Electronic*, vol. 11, July 2011.
- [12] K. S. Gallagher, “Hybrid Cars: Development and Deployment in Japan, the US and China”, 2012.
- [13] M. A. Rahman, “IPM Motor Drives for Hybrid Electric Vehicles”, *International Aegean Conference on Electrical Machines and Power Electronics*, September 2008.
- [14] K. C. Kim, C. S. Jin and J. Lee, “Magnetic Shield Design between Interior Permanent Magnet Synchronous Motor and Sensor for Hybrid Electric Vehicle”, *IEEE Transactions on Magnetics*, vol. 45, no.6, pp. 2835–2838, June 2009.
- [15] J. Malan and M. J. Kamper, “Performance of a hybrid electric vehicle using reluctance synchronous machine technology”, *IEEE Trans. Ind. Appl.*, vol. 37, no. 5, pp. 1319–1324, Sep./Oct. 2005.
- [16] E. Sulaiman, T. Kosaka, and N. Matsui, “Design and performance of 6-slot 5-pole PMFSM with hybrid excitation for hybrid electric vehicle applications”.*Power Electronics Conference (IPEC),2010 international,1962-1968*
- [17] Ying Fan, Lingling Gu, Yong Luo, Xuedong Han, and Ming Cheng “Investigation of a New Flux-Modulated Permanent Magnet Brushless Motor for EVs”, *The Scientific World Journal*, Vol. 2014, 9 pages
- [18] E. Sulaiman, T. Kosaka, and N. Matsui, “Design and analysis of high-power/high-torque density dual excitation switched-flux machine for traction drive in HEVs”, *Renewable and Sustainable Energy Reviews* 34, 517-524,2014.
- [19] A. Emadi, J. L. Young, K. Rajashekara, “Power electronics and motor drives in electric, hybrid electric, and plug-in hybrid electric vehicles”, *IEEE Trans. Ind. Electron.*, vol.55, no.6, pp.2237-2245, Jan. 2008.
- [20] D. W. Gao, C. Mi, and A. Emadi, “Modeling and simulation of electric and hybrid vehicles”, *Proc. IEEE*, vol. 95, no. 4, pp.729–745, April 2007.
- [21] R. Mizutani, “The present state and issues of the motor employed in Toyota HEVs”, *Proc. of the 29th Symposium on Motor Technology in Techno-Frontier 2009*, pp. E3-2-1-E3-2-20. (in Japanese)

- [22] T. Wang, P. Zheng, and S. Cheng, "Design characteristics of the induction motor used for hybrid electric vehicle", *IEEE Trans. Magn.*, vol. 41, no. 1, pp.505–508, Jan. 2008.
- [23] K. M. Rahman, B. Fahimi, G. Suresh, A. V. Rajarathnam, and M. Ehsani, "Advantages of switched reluctance motor applications to EV and HEV: Design and control issues", *IEEE Trans. Ind. Appl.*, vol. 36, no. 1, pp. 111–121, Jan./Feb. 2000.
- [24] X. D. Xue, K. W. E. Cheng, T. W. Ng, N. C. Cheung, "Multi-objective optimization design of in-wheel switched reluctance motors in electric vehicles", *IEEE Trans. Ind. Electron.*, vol.57, no.9, pp.2980-2987, Sept. 2010.
- [25] K. R. Geldhof, A. P. M. Van den Bossche, J. A. Melkebeek, "Rotor-position estimation of switched reluctance motors based on damped voltage resonance", *IEEE Trans. Ind. Electron.*, vol.57, no.9, pp.2954-2960, Sep. 2010.
- [26] A. G. Jack, B. C. Mecrow, and J. A. Haylock: "A comparative study of permanent magnet and switched reluctance motors for high-performance fault tolerant applications," *IEEE Trans. Ind. Appl.*, vol. 32, no. 4, pp. 889–895, Jul./Aug. 2006
- [27] M. Terashima et al., "Novel motors and controllers for high-performance electric vehicle with four in-wheel motors," *IEEE Trans. Ind. Electron.*, vol. 44, no. 1, pp. 28–38, Feb. 1997
- [28] K. T. Chau, C. C. Chan, and Chunhua Liu: "Overview of Permanent-Magnet Brushless Drives for Electric and Hybrid Electric Vehicles", *IEEE Transactions On Industrial Electronics*, Vol. 55, No. 6, June 2008
- [29] M. Zeraoulia, M. E. Hachemi: "Electric Motor Drive Selection Issues for HEV Propulsion Systems: A Comparative Study", *IEEE Transactions On Vehicular Technology*, Vol. 55, No. 6, November 2006
- [30] Z. Q. Zhu, and D. Howe: "Electrical Machines and Drives for Electric, Hybrid, and Fuel Cell Vehicles", *Proceedings of the IEEE*, Vol. 95, No. 4, April 2007
- [31] E. Sulaiman, T. Kosaka, and N. Matsui, "FEA-based design and parameter optimization study of 6-slot 5-pole PMFSM with field excitation for hybrid electric vehicle". *Power and Energy (PECon)*, IEEE International Conference on 2010, pp.206-211.
- [32] G. Dancygier and J. C. Dqlecagaray, "Motor control law and comfort law in the Peugeot and Citroën electric vehicles driven by a dc commutator motor",

- Proc. IEE—Power Electron. and Variable Speed Drives Conf., Sep. 21–23, 1998, pp. 370–374.
- [33] R. Mizutani: “The present state and issues of the motor employed in Toyota HEVs”, Proc. of the 29th Symposium on Motor Technology in Techno-Frontier, 2009.
- [34] Y. Liao, F. Liang, and T. A. Lipo: “A novel permanent magnet motor with doubly salient structure,” IEEE Trans. Ind. Appl., vol. 31, no. 5, pp. 1069–1078, Sep./Oct.1999 (bab2)
- [35] Amara, E. Hoang, M. Gabsi, M. Lecrivain, and S. Allano: “Design and comparison of different flux-switch synchronous machines for an aircraft oil breather application,” in Proc. 2nd IEEE Int. Conf. Signals, Systems, Decision and Information Technology, Mar. 2003
- [36] R. P. Deodhar, S. Andersson, I. Boldea, and T. J. E. Miller: “The flux-reversal machine: A new brushless doubly-salient permanent-magnet machine,” IEEE Trans. Ind. Appl., vol. 33, no. 4, pp. 925–934, Jul./Aug. 1997
- [37] C. Wang, S. A. Nasar, and I. Boldea: “Three-phase flux reversal machine (FRM),” IEE Proc.—Elect. Power Appl., vol. 146, no. 2, pp. 139–146, 1999
- [38] H. R. Bolton and Y. Shakweh: “Performance prediction of Laws’s relay actuator,” IEE Proc., pt. B, vol. 137, no. 1, pp. 1–13, 1990
- [39] B. C. Mecrow, T. J. Bedford, J. W. Bennet, and T. Celik: “The use of segmental rotors for 2 phase flux-switching motors,” Proc. The Int. Conf. Electrical Machines, 2006
- [40] C. Pollock and M. Wallace: “The flux switching motor, a DC motor without magnets or brushes,” in Proc. Conf. rec. IEEE IAS Annual Meeting, Vol.3, pp.1980–1987,1999.
- [41] H. Pollock, C. Pollock, R. T. Walter, and B. V. Gorti: “Low cost, high power density, flux switching machines and drives for power tools,” in Proc. Conf. Rec. IEEE IAS Annual Meeting, pp.1451–1457, 2003
- [42] C. Pollock, H. Pollock, and M. Brackley: “Electronically Controlled flux switching motors: “A comparison with an induction motor driving an axial fan”, in Proc. Conf. Rec. IEEE IAS Annual Meeting, pp.2465–2470, 2003.
- [43] Y. Amara, L. Vido, M. Gabsi, E. Hoang, A. H. Ben Ahmed and M. Lecrivain, “Hybrid Excitation Synchronous Machines: Energy-Efficient Solution for

- Vehicles Propulsion”, *IEEE Transactions on Vehicular Technology*, vol. 58, no. 5, pp.2137–2149, 2009.
- [44] J. T. Chen, Z. Q. Zhu, S. Iwasaki and R. P. Deodhar, “A Novel E-Core Switched-Flux PM Brushless AC Machine”, *IEEE Transactions on Industry Applications*, vol. 47, no. 3, May/June 2011.
- [45] J. T. Chen, Z. Q. Zhu, S. Iwasaki and R. P. Deodhar, “Comparison of Losses and Efficiency in Alternate Flux-Switching Permanent Magnet Machines”, XIX International Conference on Electrical Machines, September 2010
- [46] C. C. Chan and K. T. Chau, “An Overview of Power Electronics in Electric Vehicles”, *IEEE Transactions on Industrial Electronics*, vol. 44, no. 1, pp.3–13, February 1997.
- [47] J. T. Chen, Z. Q. Zhu, S. Iwasaki, and Rajesh P. Deodhar, “Novel Hybrid-Excited Switched-Flux Brushless AC Machine for EV/HEV Applications,” *IEEE Transactions on Vehicular Technology*, vol.60, no. 4, May 2011
- [48] E. Sulaiman, T. Kosaka, N. Matsui, and M. Z. Ahmad, “Design Studies on High Torque and High Power Density Hybrid Excitation Flux Switching Synchronous Motor for HEV Applications,” *IEEE International Power Engineering and Optimization Conferences (PEOCO2012)*, June 2012
- [49] J. Makarovic, “Lightweight positioning: design and optimization of an actuator with two-controlled degrees of freedom”, Ph.D. dissertation, Eindhoven University of Technology, the Netherlands, 2006.
- [50] E. Sulaiman, M. Z. Ahmad and Z.A. Haron, “Design Studies and Performance of HEFSM with various Slot-Pole Combination for HEV Applications,” *IEEE International Conference on Power and Energy (PECon)*, December 2012
- [51] S.N.U Zakaria and E. Sulaiman, “Performances Analysis of E-Core Hybrid Excitation Flux Switching Synchronous Motor for Hybrid Electric Vehicle,” *IEEE International Power Engineering and Optimization Conferences (PEOCO2014)*, 318-323, 24-25 March 2014
- [52] Yuksel Oguz , Mehmet Dede “Speed estimation of vector controlled squirrel cage asynchronous motor with artificial neural networks” *Energy Conversion and Management*, Vol. 52, No. 1, pp. 675-686, 2011